Efficient Nonlinear Frequency Conversion with Maximal Atomic Coherence

Maneesh Jain, Hui Xia, G. Y. Yin, A. J. Merriam, and S. E. Harris
Edward L. Ginzton Laboratory, Stanford University, Stanford, California 94305
(Received 14 June 1996)

We demonstrate efficient nonlinear frequency conversion in atomic Pb vapor under conditions where the linear susceptibility and the effective nonlinear susceptibility are of the same order. This is accomplished by using electromagnetically induced transparency to prepare a near-maximal atomic coherence on a Raman transition. This strongly driven transition is used to convert an intense laser beam from 425 to 293 nm with an efficiency of ~40%. [S0031-9007(96)01644-4]

PACS numbers: 42.79.Nv, 42.50.Gy, 42.50.Hz, 42.65.Ky

Traditional nonlinear frequency conversion processes in gases/vapors have struggled with relatively poor conversion efficiencies due to both the small magnitude of the third-order nonlinear susceptibility and the difficulty in phase matching. Efforts to increase the nonlinearity using methods such as two-photon resonance have been hindered by effects such as two-photon absorption and nonlinear phase shifts [1]. Phase matching has been an essential requirement because the physical length of the nonlinear medium required for efficient frequency conversion often greatly exceeds the coherence length.

In this Letter, we present experimental results which show how one may create a sufficiently large nonlinear polarization so as to allow efficient frequency conversion within a single (nonphase matched) coherence length. Our method relies on using electromagnetically induced transparency (EIT) to prepare a near-maximal atomic coherence on a dipole-forbidden (Raman) transition.

Figure 1(a) shows an ideal three-state atomic system. Maximal coherence on the Raman ($|1\rangle - |2\rangle$) transition is defined as $|\rho_{12}| = 0.5$. When $|\rho_{12}| = 0.5$, every atom in the sample is phase coherent with the other atoms in the sample and has equal probability amplitudes in states $|1\rangle$ and $|2\rangle$, and no probability amplitude in state $|3\rangle$. The phase coherent atoms may be viewed as a strong atomic local oscillator. The spectral components of a third laser beam beat with the local oscillator and are converted to a corresponding spectrum of sum or difference frequencies.

Following Kasapi *et al.* [2] we use EIT to prepare the atomic coherence in a sample of optically thick Pb vapor. This is accomplished by first applying the coupling laser [Fig. 1(a)], followed by the probe laser, so as to adiabatically evolve the atoms from their ground state into a phase coherent superposition of states $|1\rangle$ and $|2\rangle$. At our operating atomic density-length product, a resonant, weak-probe laser alone would see an absorption-length product of $\alpha L = 3 \times 10^5$ and a transmission of $\exp(-\alpha L)$. This large opacity is cleared by EIT, allowing undistorted image transmission through the medium [2,3].

Before describing the experiment, we will review some previous work. Tewari and Agarwal [4] first noted how phase matching in nonlinear generation can be controlled by using a resonant laser field. Harris, Field, and Imamoğlu [5] noted the possibility of greatly improved nonlinear optical processes by using EIT. The first experimental results were obtained in atomic hydrogen by Hakuta, Stoicheff, and colleagues [6]. Jain *et al.* [7] observed enhanced four-frequency mixing using EIT. High phase-conjugate gain was observed by Hemmer *et al.* [8] using coherent population trapping. The use of phase-coherent atoms for modifying the near-resonant refractive index has been studied by Scully [9]. Kochrovskaya and Mandel [10] have described the propagation of lasers in phase-coherent atomic media and Eberly *et al.* [11] have studied propagation in adiabatically prepared three-state systems.

The experimental setup in this work is similar to that of Refs. [2,3]. The two lasers in Fig. 1(a) create the large atomic coherence. The 406 nm coupling laser and the 283 nm probe laser are obtained from Ti:sapphire laser systems at 812 nm and 850 nm by frequency doubling and frequency tripling, respectively. Each of these systems is injection seeded by an external-cavity diode laser and operates in a single longitudinal mode with a long-term (one week) frequency stability of under 100 MHz [12]. The pulse durations of the probe and coupling

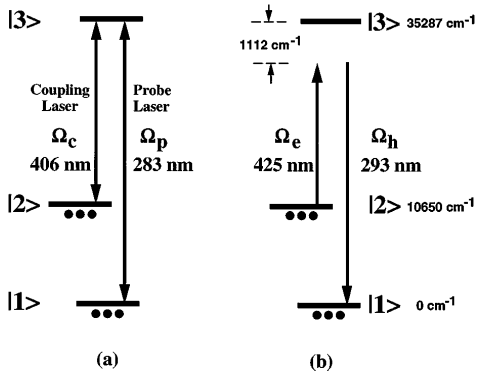

FIG. 1. (a) A large atomic coherence, ρ_{12}, is prepared by the probe laser (283 nm) and the coupling laser (406 nm). (b) The 425 nm laser mixes with the coherence in (a) to generate a sum frequency at 293 nm. $|1\rangle$, $|2\rangle$, and $|3\rangle$ denote states $6s^2 6p^2\,{}^3P_0$ (ground), $6s^2 6p^2\,{}^3P_2$, and $6s^2 6p 7s\,{}^3P_1$ of atomic ^{208}Pb.

 0031-9007/96/77(21)/4326(4)$10.00

lasers are 22 and 39 ns, and the typical pulse energies are 220 μJ and 3.2 mJ, respectively. Using a three-pass Ti:sapphire amplifier for the 812 nm laser, we are able to obtain several mJ of energy at the coupling laser. The probe laser is focused more tightly than the coupling laser, and thus the power densities for both beams in the Pb vapor cell are about 10–30 MW/cm^2. The third laser used for the four-frequency mixing experiment is chosen to be 425 nm (frequency doubled, 850 nm) [see Fig. 1(b)]. This laser has a pulse duration of 26 ns, a typical pulse energy of 400 μJ, and a power density of about 2 MW/cm^2. The generated signal at 293 nm has a pulse duration of 21 ns, a typical pulse energy of 16 μJ, and a power density of about 1 MW/cm^2. Its pulse shape is similar to that of the 425 nm pulse.

The energies of all the laser beams are measured by a Molectron (model J4-09) detector. A Coherent (model Cohu 64) high-resolution beam profiler is used to spatially align the three input beams and to measure their beam profiles at several points along the 10 in. atomic vapor cell. The average beam areas are then computed by calculating the mode volume for each beam and dividing by the cell length. These areas for the probe, coupling, and 425 nm lasers are 0.075, 0.27, and 0.63 mm^2, respectively. The area of the generated beam is inferred to be the smallest of the three input beams.

We work in 99.97% isotopically pure lead vapor (^{208}Pb) and create an ideal three-state system by using oppositely circularly polarized probe and coupling lasers. The 425 nm laser is polarized with the same helicity as the coupling laser, and the polarization of the generated beam at 293 nm is measured to be circular with the same helicity as the probe laser. We use a 10 in. long (25.4 cm) sealed fused-silica sidearm cell operating at ~940 °C at a typical atom density of about 5×10^{15} atoms/cm^3. This density is measured as in Ref. [2].

The data for this experiment is collected by fast photodetectors connected to a 5 Gsample/s Textronix TDS 684A four-channel, real-time digitizing oscilloscope which is connected to a computer running LabVIEW software. This system collects wave forms from all four channels on a shot-by-shot basis. The data is later analyzed, sorted by the timing of the probe/coupling laser input pulses, and then plotted. We discard data points where the peaks of the probe/coupling laser input pulses are separated by more than 10 ns. The data shown in Figs. 2 and 3 are from individual pulses with no averaging, while the data for Fig. 4 are averaged over 30 shots.

In this experiment, we typically generate 16 μJ of energy at 293 nm from an input energy of about 400 μJ at 425 nm. We define the term, conversion efficiency, as the ratio of the generated intensity at 293 nm to the input intensity at 425 nm *in the spatially and temporally overlapped portions of the beams.* Figure 2 shows the conversion efficiency to 293 nm as a function of the 425 nm intensity. We observe that the conversion efficiency is constant at ~40% as the 425 nm intensity is varied over about 2 orders of magnitude. The intensities of the probe and coupling lasers for this data are 12 MW/cm^2 and 30 MW/cm^2, respectively. The dephasing time γ_{21}^{-1} of the $|1\rangle$–$|2\rangle$ coherence is measured by the group delay technique of Kasapi *et al.* [2].

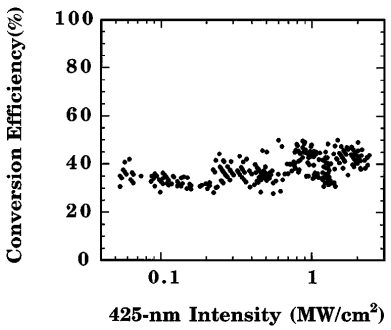

FIG. 2. Conversion efficiency vs 425 nm intensity. The conversion efficiency is constant at about ~40%. For these data, $N = 4.9 \times 10^{15} \pm 20\%$ atoms/cm^3, $\gamma_{21}^{-1} = 28$ ns, and the probe and coupling laser intensities are 12 and 30 MW/cm^2, respectively.

In Fig. 3 we show the conversion efficiency as a function of the coupling laser intensity. For this data, the intensities of the probe and 425 nm lasers are 11 MW/cm^2 and 1.9 MW/cm^2, respectively, and the cell density is $N = 3.7 \times 10^{15}$ atoms/cm^3. As the coupling laser intensity is increased from a small value, the conversion efficiency first improves linearly and then reaches a maximum value of about 39%.

In Fig. 4, we show the conversion efficiency as a function of small detunings from the two-photon resonance. The two-photon detuning is precisely controlled by very small changes in the frequency of the probe laser. At exact two-photon resonance (determined by maximizing the EIT effect for a weak probe beam), the conversion efficiency is about 10%. At a two-photon detuning of about

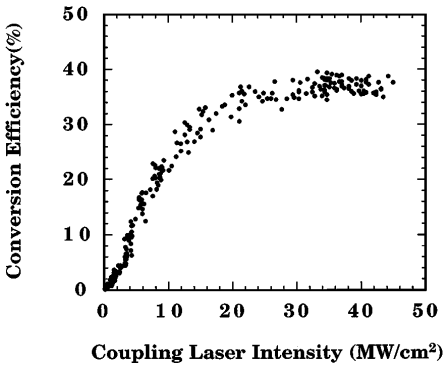

FIG. 3. Conversion efficiency vs coupling laser intensity. For these data, $N = 3.7 \times 10^{15} \pm 20\%$ atoms/cm^3, $\gamma_{21}^{-1} \sim$ 20 ns, and the probe and 425-nm laser intensities are 11 and 1.9 MW/cm^2, respectively.

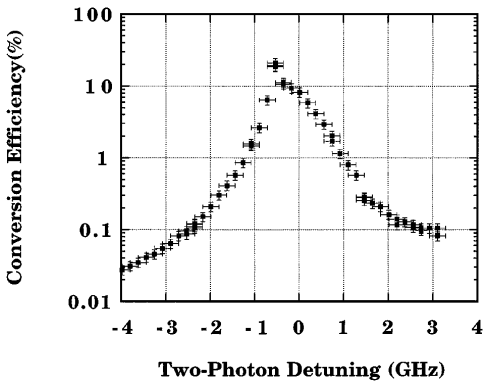

FIG. 4. Conversion efficiency vs two-photon detuning. For these data, $N = 4.9 \times 10^{15} \pm 20\%$ atoms/cm^3, $\gamma_{21}^{-1} = 14$ ns, $I_p = 13$ MW/cm^2, $I_c = 22$ MW/cm^2, and $I_e = 2.8$ MW/cm^2. The maximum conversion efficiency is ~20%.

-0.5 GHz, we achieve a conversion efficiency of about 20%. Small detunings from two-photon resonance affect the phase of the probe and coupling lasers, thereby allowing us to compensate for a small phase mismatch. The data for Figs. 2 and 3 are collected at the optimal two-photon detuning.

We now turn to a theoretical discussion of this work. We consider a three-state system in the rotating wave approximation and ignore the interaction of the probe and 293 nm lasers with the $|2\rangle$–$|3\rangle$ transition and the coupling and 425 nm lasers with the $|1\rangle$–$|3\rangle$ transition. We assume an undepleted atomic coherence, ρ_{12}. Writing the Rabi frequency of the ith field as $\Omega_i(z)\exp(-jk_iz)$, the propagation equations for a frequency converter from $\Omega_e(z)$ to $\Omega_h(z)$ are

$$\frac{d\Omega_e}{dz} = -j\beta_e\rho_{21}\Omega_h(z)\exp(+j\Delta kz), \quad (1)$$

$$\frac{d\Omega_h}{dz} = -j\beta_h\rho_{12}\Omega_e(z)\exp(-j\Delta kz), \quad (2)$$

where $\Delta k = (k_{12} + k_e - k_h)$ and $k_{12} = (k_p - k_c)$ is the k vector of the atomic coherence. $\beta_e = \omega_e N|\mu_{23}|^2/2\epsilon_0 c\hbar\Delta\omega_3$ and $\beta_h = \omega_h N|\mu_{13}|^2/(2\epsilon_0 c\hbar \times \Delta\omega_3)$, where $\Delta\omega_3$ is the common detuning of the two fields from state $|3\rangle$. The quantities k_p, k_c, k_e, and k_h are defined to include only atomic contributions. For copropagating fields in free space, $\Delta k = 0$. With the boundary condition $\Omega_h(0) = 0$, the solutions to Eqs. (1) and (2) are

$$\Omega_e(z) = \Omega_e(0)\exp(+j\Delta kz/2) \times [\cos(sz) - j(\Delta k/2s)\sin(sz)], \quad (3)$$

$$\Omega_h(z) = -j\Omega_e(0)\exp(-j\Delta kz/2)[(\beta_h\rho_{12}/s)\sin(sz)], \quad (4)$$

where $s^2 = (\Delta k/2)^2 + \beta_e\beta_h|\rho_{12}|^2$. We note from Eq. (3) that large conversion from Ω_e to Ω_h requires $(\Delta k/2s) \ll 1$. When $|\rho_{12}|$ is small, this condition imposes a stringent phase matching requirement; if $|\rho_{12}|$ is made large, the phase matching requirement is greatly alleviated.

In this work, phase matching is accomplished by adjusting the k vector, k_{12}, of the atomic coherence using a small two-photon detuning, $\Delta\omega_2$. One may show that, for small $\Delta\omega_2$, $k_p \propto -\Delta\omega_2$ and $k_c \propto +\Delta\omega_2$; hence, $k_{12} = (k_p - k_c) \sim -\Delta\omega_2$. For the conditions of Fig. 4 ($\Omega_p = 3$ cm^{-1} and $\Omega_c = 6$ cm^{-1}), we find that the phase shift of the atomic coherence is $k_{12}L = +\pi$ when $\Delta\omega_2 \sim -0.3$ GHz. Hence, we may correct for a small phase mismatch by a very small two-photon detuning and no external phase matching agent is necessary.

For a phase matched interaction ($\Delta k = 0$) with maximal coherence ($|\rho_{12}| = 0.5$), the density-length product required for complete conversion from Ω_e to Ω_h has a minimum value determined by $\sqrt{\beta_e\beta_h}L = \pi$. The density-length product used in this experiment is close to this value.

We next discuss numerical simulations of the experiment. We assume monochromatic fields and work with a 3×3 Hamiltonian which includes all four fields. The essential idea is that if the dephasing of the $|1\rangle$–$|2\rangle$ transition is neglected, we may take the atomic state vector to be in a single eigenvector of the Hamiltonian. The dipole moment is computed from the components of this eigenvector, averaged over the Doppler distribution, and used to drive Maxwell equations. The modified fields are used to update the Hamiltonian and the process is iterated. Figure 5(a) shows the conversion efficiency as a function of two-photon laser detuning. A small, negative two-photon detuning maximizes the conversion efficiency, in agreement with Fig. 4. The peak conversion efficiencies predicted are a factor of 3 higher than those observed experimentally. We believe that this is due to the neglect of the dephasing of the atomic coherence in this simulation.

To investigate the effect of dephasing on the atomic coherence, we performed a separate numerical simulation to solve the density matrix equations for a three-level atomic system interacting with pulsed laser fields (propagation effects were ignored). The results of this simulation are shown in Fig. 5(b). In the absence of dephasing ($\gamma_{21} = 0$), maximal atomic coherence, $|\rho_{12}| = 0.5$, is achieved. Dephasing of the $|1\rangle$–$|2\rangle$ transition reduces the magnitude of the atomic coherence.

Although the conversion efficiency from 425 to 293 nm of the temporally and spatially overlapped portions of the beams is approximately 40%, the overall efficiency, including the intensities of all beams, is 2.3%. This problem can be solved by increasing the 425-nm intensity and by using intracavity operation to enhance the intensity of the 406-nm radiation. The 406-nm field is generated and not depleted during the conversion process.

We summarize the requirements for a nonlinear frequency converter which uses EIT to create a near-maximal

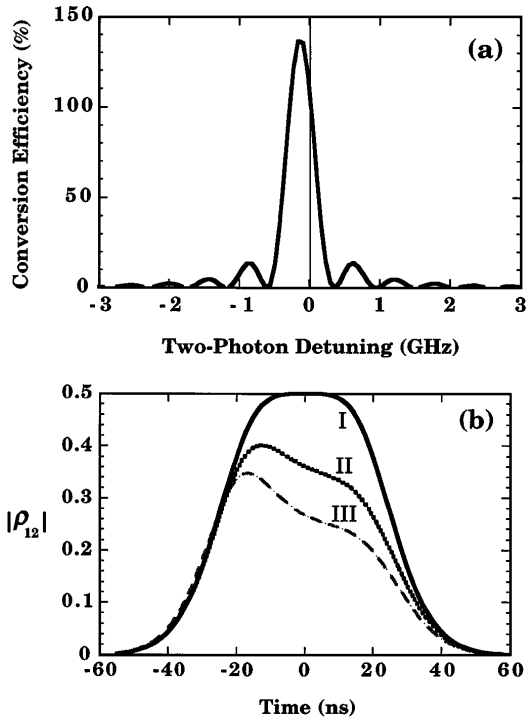

FIG. 5. Numerical simulations. (a) Conversion efficiency vs two-photon laser detuning. The conditions for this simulation are the same as Fig. 4. Other parameters are two-photon Doppler width $= 0.02\ \mathrm{cm}^{-1}$, single-photon Doppler width $= 0.06\ \mathrm{cm}^{-1}$, and $2\gamma_3 = 0.002\ \mathrm{cm}^{-1}$ (at unity photon-to-photon conversion, the intensity conversion efficiency may exceed 100%). (b) The effect of dephasing, γ_{21}, on $|\rho_{12}|$. For this simulation, the probe pulse duration $= 22$ ns, the coupling pulse duration $= 39$ ns, and $\Omega_p = \Omega_c = 3\ \mathrm{cm}^{-1}$. (I) $\gamma_{21} = 0$, (II) $\gamma_{21}^{-1} = 28$ ns, and (III) $\gamma_{21}^{-1} = 14$ ns.

atomic coherence: (1) It is essential that the pulse duration of the probe laser be shorter than (or not substantially exceed) the dephasing time of the coherence. (2) The intensity of the coupling laser must be sufficiently large so that its Rabi frequency exceed the inhomogeneous linewidth of the $|1\rangle - |2\rangle$ transition. (3) To allow sufficient time for preparation, the number of photons in the coupling laser pulse must exceed the oscillator strength weighted number of atoms in the laser path [13].

We have shown how to perform efficient frequency conversion by using a near-maximal atomic coherence prepared by EIT. This method allows conversion efficiencies very much larger than those obtained by traditional nonlinear optical techniques. Extensions to the vacuum ultraviolet and the infrared regions of the spectrum are likely.

The authors thank A. Kasapi for his contributions and S. M. Hooker for helpful discussions. The work was supported by the Office of Naval Research, the U.S. Air Force Office of Scientific Research, and the U.S. Army Research Office.

[1] J. F. Reintjes, *Nonlinear Optical Parametric Processes in Liquids and Gases* (Academic Press, Orlando, FL, 1984), pp. 252–278.
[2] A. Kasapi, M. Jain, G. Y. Yin, and S. E. Harris, Phys. Rev. Lett. **74**, 2447 (1995); A. Kasapi, G. Y. Yin, M. Jain, and S. E. Harris, Phys. Rev. A **53**, 4547 (1996).
[3] M. Jain, A. J. Merriam, A. Kasapi, G. Y. Yin, and S. E. Harris, Phys. Rev. Lett. **75**, 4385 (1995).
[4] S. P. Tewari and G. S. Agarwal, Phys. Rev. Lett. **56**, 1811 (1986).
[5] S. E. Harris, J. E. Field, and A. Imamoğlu, Phys. Rev. Lett. **64**, 1107 (1990).
[6] K. Hakuta, L. Marmet, and B. P. Stoicheff, Phys. Rev. Lett. **66**, 596 (1991); G. Z. Zhang, K. Hakuta, and B. P. Stoicheff, Phys. Rev. Lett. **71**, 3099 (1993).
[7] M. Jain, G. Y. Yin, J. E. Field, and S. E. Harris, Opt. Lett. **18**, 998 (1993).
[8] P. R. Hemmer, D. P. Katz, J. Donoghue, M. Cronin-Golomb, M. S. Shahriar, and P. Kumar, Opt. Lett. **20**, 982 (1995).
[9] M. O. Scully, Phys. Rev. Lett. **67**, 1855 (1991).
[10] O. Kocharovskaya and P. Mandel, Phys. Rev. A **42**, 523 (1990).
[11] J. H. Eberly, A. Rahman, and R. Grobe, Phys. Rev. Lett. **76**, 3687 (1996); R. Grobe, F. T. Hioe, and J. H. Eberly, Phys. Rev. Lett. **73**, 3183 (1994).
[12] A. Kasapi, G. Y. Yin, and M. Jain, Appl. Opt. **35**, 1999 (1996).
[13] S. E. Harris and Zhen-Fei Luo, Phys. Rev. A **52**, R928 (1995).